



Application of artificial intelligence methods during the processing of spatial data from the hydrographic systems for coastal zone

Marta Włodarczyk-Sielicka¹, Robertas Damaševičius²

¹Maritime University of Szczecin, Faculty of Navigation, Department of Hydrography and Spatial Analysis, Waly Chrobrego 1-2, Szczecin, 70-500, Poland

²Vytautas Magnus University, Faculty of Informatics, Department of Applied Informatics, Universiteto str. 10–202, 53361 Akademija, Kaunas District, Lithuania

Correspondence to: Marta Włodarczyk-Sielicka (m.wlodarczyk@pm.szczecin.pl)

Abstract. Effective processing of spatial data in coastal zones requires the integration of measurements from various sensors to achieve a more comprehensive picture of dynamic environmental changes. This study proposes a new approach to spatial data analysis, combining information from the LiDAR system and multi-beam echo sounder (MBES). This combination of both sources allowed for a more accurate estimation of the topography and bathymetry of the coastal zone. A key element of the study was developing an original data reduction method based on Self-Organizing Maps (SOM) neural networks. Initially used for analysing bathymetric data, this method has been optimised for aquatic data, enabling effective processing of both heights from LiDAR and depths from MBES. Data reduction significantly shortened computation time – interpolation using the Empirical Bayesian Kriging (EBK) method for raw data took over 9 hours, whereas, for the reduced data (those with the highest density), it took just 4 minutes and 51 seconds while maintaining the comparable quality of results. The study confirmed that the reduced data meets the requirements of the International Hydrographic Organization (IHO) for shallow water bodies, which indicates the high accuracy of the method employed. The results suggest that data reduction based on artificial intelligence allows for the efficient management of big spatial data, and its integration with classical GIS interpolation methods can find broad applications in hydrography, environmental monitoring, and coastal zone management.

1 Introduction

It is essential to address and analyse the harmful consequences arising from the economic use and exploitation of resources found in the coastal zone. This area and the detailed analysis of its changes are significant for many aspects, such as ecological integrity, rational development organisation, and sustainable management. Artificial intelligence systems carry out various tasks and functions, including autonomous image interpretation, geospatial analysis, real-time monitoring, and management of complex technical systems (Vitousek S. et al., 2023). Artificial intelligence is developing rapidly. The advancement of intelligent spatial data processing tools enables researchers to conduct detailed data analyses, including their understanding. Thanks to machine learning algorithms, such as neural networks, it is possible to identify key areas for



protection and predict changes in coastal zones (Zhao, Q. et al., 2023). Gathering spatial data in coastal zones is crucial for monitoring and managing these dynamic areas. Spatial data obtained in coastal zones can be collected using various modern systems. Different technologies provide precise information about topography, bathymetry, and environmental changes.

35 Spatial data in coastal zones is characterised by a high ecological dynamism and continuous changes resulting from natural processes such as erosion, sedimentation, and sea level changes. These areas encompass various ecosystems, including beaches, dunes, wetlands, and port areas like quays, which require diverse data collection methods. This article focuses on point clouds from Lidar Detection and Ranging (LiDAR) systems and bathymetric data obtained from multibeam echosounders. LiDAR technology enables rapid and accurate acquisition of data on the coastal terrain. It is beneficial for

40 mapping large areas and monitoring morphological changes along the coast (Irish J.L. 1998). Bathymetric data gathered using multibeam echosounder (MBES) systems play a key role in mapping the sea floor, providing high-resolution information about its topography. In recent years, this technology has been applied in various scientific and practical studies (Foglini, F. et al. 2025).

1.1 Spatial data processing in the coastal zone

45 Spatial data processing in coastal zones is crucial for monitoring and managing these dynamic areas. In recent years, the development of remote sensing technology and data analysis methods has enabled more precise and efficient research in these regions. In 2020, a study was published regarding applying deep learning-based interpolation methods for coastal bathymetry. The authors presented techniques using deep neural networks to estimate bathymetry based on sparse, multi-scale measurements, allowing for more accurate seabed maps than traditional methods (Qian, Y. et al. 2020). Another

50 example of the significance of this issue is an article on identifying shoreline zones and three-dimensional coastal mapping using uncrewed aerial vehicles (UAVs). The study showcased a methodology for acquiring and processing high-resolution data for coastal zones using a UAV equipped with a small commercial camera. The proposed method integrates computer vision algorithms for 3D representation with image processing techniques for analysis (Papakonstantinou, A. et al. 2016). Another example is the study regarding spatial data infrastructure for coastal environments. The central focus of this chapter

55 is the review and discussion of the data portal as a fundamental means for searching, discovering, and retrieving spatial data (Wright, D.J. 2009). In 2020, a publication regarding Marine Spatial Data Infrastructure (MSDI) was released. It discusses the key elements of MSDI and its significance in processes such as marine spatial planning and coastal zone management. MSDI extends traditional Spatial Data Infrastructure (SDI) into the marine environment. Its goal is to facilitate hydro-spatial data discovery, access, management, distribution, reuse, and archiving. MSDI provides timely access to data from various

60 public and private organisations related to marine fields, such as hydrography, oceanography, and meteorology. This data is used in applications related to navigation safety, marine activities, economic development, scientific research, and sustainable management of marine ecosystems. Implementing MSDI is crucial for the effective management of marine data and for supporting the sustainable development of marine areas (Contarinis S. et al., 2022). Another example is the study concerning creating an online interactive map depicting projected sea level rise along the northern coastline of Vancouver.



65 This study highlights the importance of visualisation in educating coastal communities about potential climate change-
related threats (DiPaola, F. et al., 2023). Processing spatial data in coastal zones from hydrographic systems is also crucial
for understanding and managing these dynamic areas. Specht and Wiśniewska presented a method for developing a Digital
Terrain Model (DTM) of the coastal zone based on topo-bathymetric data from remote sensing sensors. Research conducted
in the area of the mouth of the Wisla Smiala in Gdansk showed that the use of images from uncrewed aerial vehicles (UAV)
70 and the Support Vector Regression (SVR) algorithm allows for achieving high accuracy in the terrain model, meeting the
requirements of the International Hydrographic Organization (IHO) for shallow water bodies (Specht, M. et al. 2024). In
2025, NV5 and NOAA celebrated 20 years of collaboration on geospatial mapping projects of the coasts and waterways of
the United States. Modern measurement technologies, such as multibeam echosounders and innovative data processing
approaches, have provided valuable insights supporting marine mapping, resource management, and a better understanding
75 of the changing coastal environment (NV5 and NOAA, 2025). In 2023, the third edition of the IHO C-17 publication
"Spatial Data Infrastructures: The Marine Dimension" was released, explaining why and how hydrographic offices should
develop, support, and promote MSDI. This document highlights the importance of standardisation and interoperability of
hydrographic data in the context of spatial planning of marine areas and managing the coastal zone (IHO, 2023). The above
examples emphasise the significance of modern technologies and analytical methods in processing spatial data in coastal
80 zones, contributing to better understanding and managing these key areas.

1.2 Fundamentals of artificial intelligence in geospatial analysis

Artificial intelligence (AI) plays an increasingly significant role in processing spatial data, introducing advanced methods of
analysis and interpretation of geographical information. There are studies regarding the use of AI techniques in analysing
spatial data, highlighting the potential of these methods to improve the accuracy and efficiency of processing geographical
information (Rane, J. et al. 2024). Integrating AI with GIS enables advanced spatial analysis, particularly useful in urban
85 planning, natural resource management, and environmental change monitoring. An interesting article has been published
discussing the synergy between these technologies and their application in security operations, from surveillance to disaster
response (Lugga, M. S. 2025). In 2023, a review was published on the methods, applications, and ethics associated with the
use of AI in cartography, emphasising the rapid development of geospatial artificial intelligence (GeoAI) and its potential in
90 automating cartographic tasks and introducing new ways of creating maps (Kang, Y. et al. 2024). AI is widely used to detect
and classify objects in LiDAR data. A study published in 2023 presented a system using LiDAR sensors to capture dynamic
point cloud data in industrial environments and interpret these scenes using AI algorithms for object detection. This detection
allows for differentiation between people and other moving objects in areas of safety significance. Several AI methods
relevant to such applications were analysed (Poenicke, O. et al. 2023).

95 The analysis of hydrographic data encompasses various methods that have evolved in recent years due to technological
advancements and the increasing availability of data (Biernacik P. et al., 2023). One of the key approaches is the application
of deep learning methods for interpolating bathymetry in coastal zones. Techniques based on deep learning have already



been proposed for estimating bathymetry from sparse, multi-scale measurements, demonstrating superiority over traditional kriging methods in identifying structures with sharp gradients (Qian Y. et al., 2020). Another approach is the use of functional data analysis to investigate oceanographic parameters. Other researchers have applied functional kriging methodology to estimate temperature and salinity as functions of depth, enabling the attainment of more precise profiles of these parameters compared to traditional point methods. (Yarger D. et al. 2020).

As technology advances, the integration of AI in the processing of spatial data is becoming increasingly sophisticated, offering new opportunities for analysing and interpreting complex geographical datasets. Artificial intelligence is growing in processing bathymetric data derived from multibeam echosounders. The integration of AI techniques with traditional analysis methods enables the automation of processes, enhancing accuracy and efficiency in seabed mapping. Modern multibeam echosounders generate vast amounts of data, posing challenges in effective processing. Minelli et al. (2021) developed a semi-automated data processing system that combines traditional analysis methods with semi-supervised machine learning. This system improves efficiency and reliability in detecting and classifying targets in water column data, such as fish schools or gas leaks (Minelli, A. et al. 2021). Deep learning techniques are employed for the segmentation and classification of objects in MBES data. Christensen and other authors applied neural networks to segment fish in echosounder images, achieving high effectiveness even under low-quality data conditions (Christensen J. H. et al. 2020). Another topic is the automatic cleaning of multibeam echosounder data, which is crucial for ensuring their quality. Le Deunf reviewed bathymetric data cleaning methods, highlighting the importance of anomaly detection algorithms in automating this process. (Le Deunf J. et al. 2020). AI can also be utilised to optimise underwater mapping. This includes developing MBES data processing systems that integrate sonar parameter configuration, data storage, and real-time processing modules. This approach enables more efficient and accurate seabed mapping (Zhang, F. et al. 2024). Despite numerous benefits, the integration of AI in MBES data processing presents challenges, such as ensuring data quality, the interpretability of AI models, and the need for large datasets to train the models. The application of artificial intelligence in processing data from multibeam echo sounders contributes to more efficient and precise seabed mapping, opening new opportunities in hydrographic research and marine operations. The research in this article focuses on the application of AI to process data from LiDAR and MBES systems for quicker and more efficient analysis. The use of AI proposed in this publication will allow for effective reduction and simultaneous integration of selected spatial data sources to achieve more comprehensive analyses.

Contemporary methods of processing spatial data in coastal zones require effective integration of information from various sensors to obtain a comprehensive picture of the dynamic processes occurring in these areas. Traditional approaches to data analysis often focus on individual measurement sources, which can limit the accuracy and precision of mapping terrain structures. This study proposes a new approach to spatial data analysis based on the integration of two different measurement technologies – LiDAR and multi-beam echolocation (MBES). By combining and processing data from both systems, achieving a more detailed analysis of the topography and bathymetry of the coastal zone was possible.



One of the key aspects of the study was the development of an original method for reducing spatial data, utilising Self-Organising Maps (SOM) neural networks. Initially, this method was primarily applied to the analysis of bathymetric data; however, within this research, it has been optimised for processing water-column data, allowing practical application for both elevation values from LiDAR and depth values from MBES. By appropriately adapting the algorithm to data with positive and negative values, the developed method enables efficient and precise processing of large datasets of spatial information. This represents a significant extension of existing data analysis methods in coastal areas, opening up new possibilities for monitoring environmental changes, managing port infrastructure, and modelling geomorphological processes.

2 Study Area and Data

The test area is located in the port of Szczecin, one of Poland's largest seaports, situated on the Oder River, approximately 65 km from the Baltic Sea. Together with the port in Swinoujscie, it forms the Szczecin- Swinoujscie Port Complex, which plays a key role in maritime trade and cargo handling. It mainly handles general cargo, containers, coal, metal ores, and agricultural products. It is also an important logistics hub and has a modern cargo-handling infrastructure. The test area includes a coastal zone that is one hundred metres wide and one hundred and fifty metres long. The water zone includes an area of reinforced quay along with port infrastructure, while the underwater zone encompasses the seabed area. The extent of the test area is presented in Figure 1.

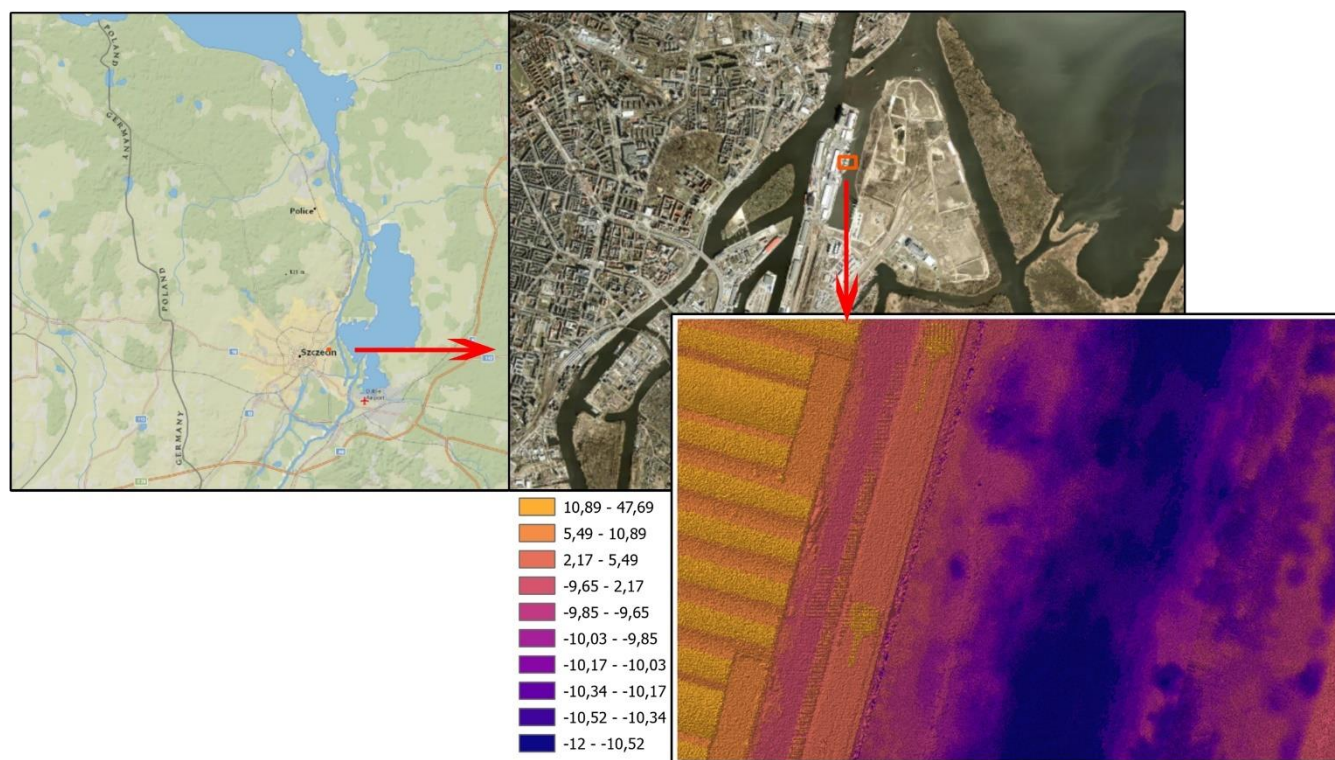


Figure 1: Test area. Study area map prepared by the author using their own data and basemap layers (Topographic and Imagery) from ArcGIS Pro. Basemap sources: © Esri, HERE, Garmin, FAO, NOAA, USGS, NGA, EPA, NPS.

The coastal area from which data was collected using LiDAR and multibeam echosounders includes land and seabed. LiDAR (Light Detection and Ranging) allowed for detailed imaging of the terrain above water, including the coastline, beaches, cliffs, and port infrastructure. Meanwhile, the multibeam echosounder (MBES) enabled precise seabed mapping, detecting its structure, depth, and potential navigational hazards. By combining these technologies, a comprehensive area model was obtained, which is useful for analysing environmental changes, engineering planning, and ensuring navigational safety. The collected data was processed, combined into a single dataset, and converted to XYZ format. The first two columns represent the position of each point, while the third column shows the height or depth of the area. The data was processed in UTM 84 – 33N format. The dataset consists of 2,168,011 measurement points. The average Z value is -9.18, suggesting that most points are below the water level. The standard deviation is 4.16, indicating moderate variability in depth values. The minimum value is -12, suggesting the deepest measured points, and the first quartile (25%) has a value of -10.34, indicating that a significant portion of the data relates to areas with depths greater than 10 metres. A total of 115,475 points, or 5.33% of all data, are above sea level, indicating that they encompass coastal land areas. The average height is 7.60 metres. The standard deviation in this case is 4.97, indicating considerable variability in heights, covering both low coastal areas and higher land features, in this case, port cranes. The minimum height is 0.02, indicating that some points are close to



the reference level. The first quartile (25% of the data) has a value of 2.36, which indicates that one in four points above zero has a height of less than 2.36 metres.

This huge amount of data can be classified as spatial big data. Especially the data obtained using the multibeam echosounder MBES (Mujta W. et al., 2023). Data reduction is a crucial process in spatial analysis. Large datasets require significant computational resources for analysis, visualisation, and modelling. Reducing the number of points considerably speeds up computations and decreases hardware requirements. An excessive number of points in 3D models or maps can cause difficulties with their display and interpretation. Data reduction allows for the retention of the most important features of the surface, eliminating redundant information that may burden graphics and visual analysis. Excessing points can also lead to unnecessary detail, which is not always needed in analyses. Reducing data or simplifying its structure enables easier analysis of elevation trends and seabed structure. Additionally, storing and transmitting large datasets can be problematic, particularly in the context of GIS systems, cloud computing, and 3D modelling. In summary, XYZ data reduction allows for work optimisation, better data management, improved quality of analyses, and accelerated computations and visualisations. As a result, future analyses will be more efficient, accurate, and easier to interpret.

3 Methodology

An original model was used during the research to reduce data from a multibeam echosounder. The reduction method allows for the retention of source data without generalisation. This method was developed to create hydrographic charts. During this research, it was optimised for application in processing data from LiDAR systems. The optimisation involved adjusting the method for positive elevation data and negative depth data. Previous use of the method focused solely on depth-related data. The entire algorithm was implemented in the Matlab environment. The input data for the method were a combined XYZ dataset from the coastal area, which encompasses the port area and the seabed surface. The method employs Self-Organising Maps (SOM) developed by Teuvo Kohonen. It is used for analysing and clustering multidimensional data, including spatial data. SOM transforms complex, multidimensional data into a two-dimensional grid of neurons while preserving the topological relationships between the data (Augustijn, EW. et al., 2013). Network structure: SOM consists of a two-dimensional grid of neurons, where each neuron is represented by a weight vector with the same number of dimensions as the input data (Tripathi, K. 2024). Figure 2 illustrates the fundamental structure of a Self-Organising Map.

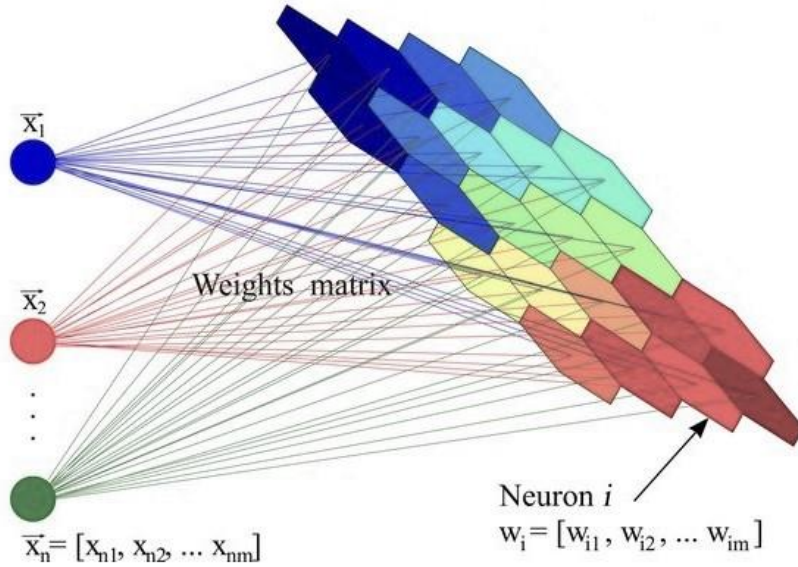


Figure 2: Basic structure of Self-Organizing Map.

During the training process, the distance between the input data vector and the weight vectors of all neurons is calculated for each input data vector. The neuron with weights closest to the data vector is selected as the winner. The weight vectors of the winner and its neighbours are updated towards the data vector, allowing the network to adapt to the structure of the input data. Once the learning process is complete, similar input data is mapped onto neighbouring neurons in the grid, facilitating the identification of clusters and patterns in the data.

During the learning process, the weights of the neurons are updated towards the input data vector. The formula for updating the weights for neuron v in iteration s is as follows Eq. (1):

$$W_v(s+1) = W_v(s) + \theta(u,v,s) * \alpha(s) * (D(t) - W_v(s)) \quad (1)$$

Where:

$W_v(s)$ – neuron weight vector v in the iteration s ,

$D(t)$ – input data vector over time t ,

$\alpha(s)$ – learning rate in the iteration s ,

$\theta(u,v,s)$ – neighbourhood function defining the influence of a neuron u (best fitted) to the neuron v in the iteration s .

The neighbourhood function $\theta(u,v,s)$ defines the degree of interaction between neurons and typically decreases with the distance between them on the map and over time. A commonly used function is the Gaussian function. The learning rate $\alpha(s)$ controls the rate of adaptation of weights and usually decreases as the learning process progresses. An example relationship

is represented by the formula Eq. (2):

$$\alpha(s) = \alpha_0 * \exp\left(-\frac{s}{T}\right) \quad (2)$$



Where:

α_0 – initial learning rate,

T – time constant determining the rate of decline.

- 215 The above relationships describe the fundamental mechanisms of adaptation in self-organising maps, allowing the model to learn and organise input data unsupervised (Asan, U. et al. 2012).

The author's method of spatial data reduction using SOM represents a very good tool for exploring and analysing spatial data. It allows for effective clustering and data reduction, as well as a subsequent faster visualisation.

- 220 The entire reduction process consists of three main stages: initial division of geospatial data into smaller subsets – preprocessing, clustering of data using artificial neural networks, and selection of the point or points with minimal depth/height for the given subset. The following configurations of self-organising map parameters were chosen as optimal for further research: hexagonal topology, initial neighbourhood size of 10, Euclidean distance, number of iterations set at 200, and the WTM rule.

- 225 Additionally, the authors employed the Empirical Bayesian Kriging (EBK) interpolation method, which is implemented in ArcGIS Pro software. This advanced kriging method combines a statistical approach to interpolation with the automatic fitting of variogram models. EBK is particularly useful when spatial data is limited, unevenly distributed, or exhibits local variability. The EBK method analyses the input data and its spatial distribution. In the next step, EBK divides the data into smaller groups and automatically fits a variogram model for each of them. Unlike classical kriging, EBK does not assume a
230 single global variogram for the entire area in advance. Variograms are estimated iteratively and locally. The method generates multiple variograms to account for uncertainty in the estimation of variograms (based on the assumed error distribution). For each variogram, Monte Carlo simulations are conducted. The results of these simulations allow for consideration of both the uncertainty of the variogram and that of the interpolation itself. Based on the fitted models and simulation results, the method interpolates values onto the output grid (Zaresefat, M. et al. 2024).

- 235 The EBK method is not strictly an AI method but can be perceived as an intelligent approach. EBK automatically adjusts the variogram models, eliminating the need for manual definition. As a result, the method appears intelligent, but this is due to well-designed statistical algorithms rather than AI. Variograms are fitted locally, which allows the method to perform well with irregular data. Through iterative processes and simulations, the method handles large and complex datasets.

The overall methodology of the research is presented in Figure 3.

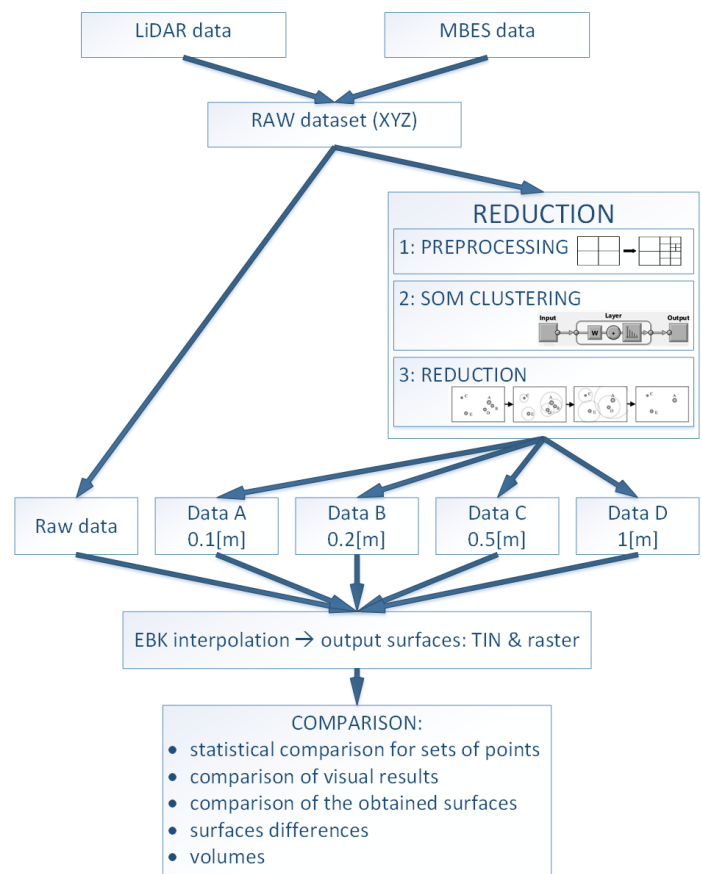


Figure 3: General scheme of the research methodology.

Firstly, the data obtained from measurement systems was appropriately processed and combined into a single dataset. The data from the terrestrial zone has positive Z values – heights, while the data from the underwater zone has negative Z values - depths. In the next step, the data was reduced using a method developed by the author, employing AI. The reduced source data used four resulting densities. The authors assumed that the output data should be close to the following resolutions for the SOM clusters: 0.1m, 0.2m, 0.5m, and 1m. The reduced output datasets were named Data A, B, C, and D. In the next step, both the source and the reduced data were processed using the EBK interpolation method, resulting in surfaces in TIN models and raster models. In the final step, all results were subjected to detailed comparative analysis.

4 Results

In the first step, it is necessary to present the statistics related to the generated sets of points after reduction. Table 1 presents all statistical data for the obtained results: for raw data, before reduction, and for reduced sets designated as data A (sets reduced in the range of 0.1m), data B (sets reduced in the range of 0.2m), data C (sets reduced in the range of 0.5m), and



data D (sets reduced in the range of 1m). The table includes the total number of observations, mean value, standard
255 deviation, minimum and maximum values, and individual quartiles.

Table 1. Statistics for reduced datasets.

| | COUNT | MEAN [m] | STD | MIN [m] | 25% | 50% | 75% | MAX [m] |
|----------|---------|----------|------|---------|--------|--------|-------|---------|
| raw data | 2168011 | -9,18 | 4,16 | -12,00 | -10,34 | -10,10 | -9,85 | 47,69 |
| data A | 510531 | -6,66 | 7,28 | -11,65 | -10,21 | -9,94 | -9,58 | 47,69 |
| data B | 269700 | -5,67 | 7,98 | -11,42 | -10,16 | -9,85 | -7,89 | 47,69 |
| data C | 64052 | -3,85 | 8,94 | -11,28 | -10,05 | -9,67 | 2,45 | 47,69 |
| data D | 18107 | -3,56 | 9,14 | -11,08 | -9,97 | -9,57 | 2,52 | 47,69 |

The raw data comprises over 2 million points with an average value of -9.18 m and a relatively small standard deviation of
260 4.16 m. The lowest value is -12 m, while the highest is 47.69 m. The quartiles suggest that most of the data is concentrated
around negative values. Dataset A contains 510531 points, has a higher average (-6.66 m), and a larger standard deviation
(7.28 m), indicating a greater dispersion of data. The minimum and maximum heights remain similar to those in the raw
data. Dataset B includes 269700 points and is characterised by an even higher average (-5.67 m) and a larger standard
deviation (7.98 m). The first quartile (-10.16 m) and median (-9.85 m) suggest that, compared to dataset A, a slightly greater
265 number of values lie within the higher ranges. Dataset C contains significantly fewer points (64052) and stands out with an
average of -3.85 m and an even more significant standard deviation (8.94 m). Notably, the third quartile reaches a positive
value (2.45 m), indicating that a substantial portion of the data begins to encompass positive heights as well. The smallest
dataset, Dataset D, consists of 18107 points and averages -3.56 m, with the most significant standard deviation (9.14 m)
among all the datasets. Similar to Dataset C, the quartiles indicate a wider spread of values, with the third quartile at 2.52 m
270 suggesting that this subset contains even higher values. Generally, as the number of points is reduced in successive datasets,
the average height increases, and the spread of the data becomes more considerable. This indicates a selection of points such
that lower values are eliminated, leaving behind a more varied subset shifted towards higher values. This closely relates to
the fact that there were significantly more points with negative heights (points collected using MBES) than points from the
LiDAR system. The data were also analysed using the Distribution of Z Values Across Models in the form of a boxplot,
275 which has been shown in Figure 4.

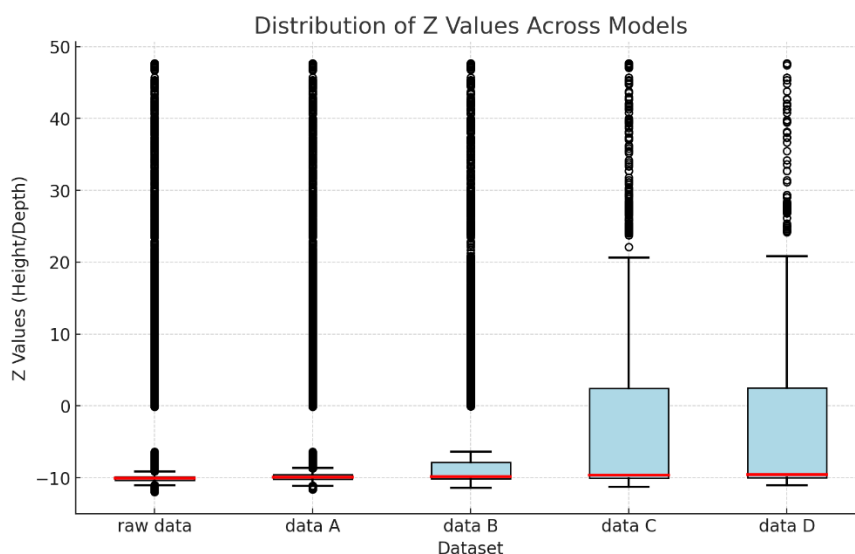


Figure 4: Distribution Of Z Values Across Models.

The graph depicts the distribution of the values Z, representing heights and depths, for the respective data sets. It shows how the individual sets differ in terms of median, range, and outliers. The raw data set contains the largest amount of data, as can be observed from the width of the box. The median is close to negative values, suggesting that most points represent water depths. The range of values is very wide, encompassing both the deepest underwater points and the highest points on land. Numerous outliers are also visible in the upper range, indicating isolated, exceptionally high terrain points. In the subsequent data sets, from data A to data D, a gradual shift of the median towards higher values can be observed, meaning that during the selection process, more and more underwater points were eliminated, leaving those located on land. In data A, the negative range of values still predominates, but the data range is slightly smaller than in the raw data. In data B, the lower quartile shifts upwards, while the upper quartile starts to include more positive values, suggesting a more balanced distribution between land and water points. In data C, the median is already approaching positive values, and the upper quartile clearly exceeds 0 m, indicating that there are increasingly more land points in the data set. In data set C (the most reduced), most values are already above 0 m. The median and quartiles have clearly shifted upwards, indicating that the water depths have been almost entirely removed from this set. Outliers are visible in both the lower and upper ranges; however, the set is most concentrated around land elevations. The outliers in the highest ranges may represent exceptionally high terrain features, such as loading cranes.

The next diagram presents statistical values such as the average, standard deviation, minimum, and maximum for five different datasets (Figure 5).

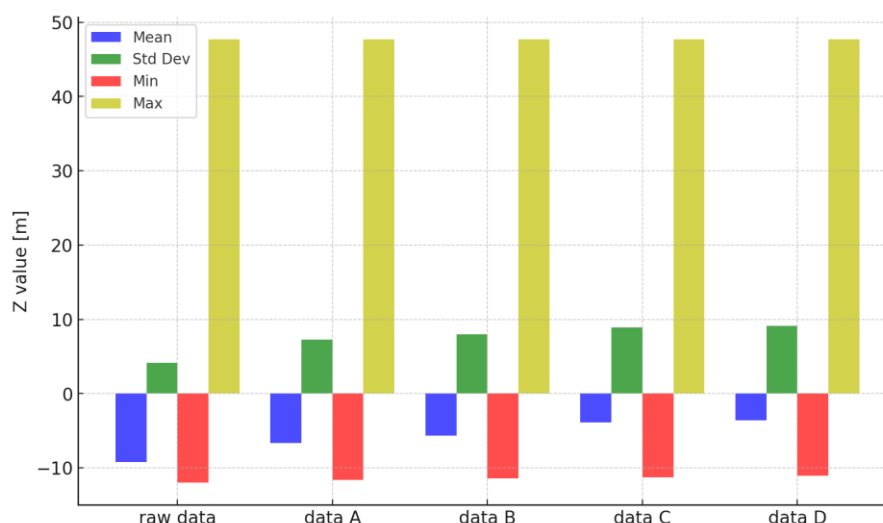


Figure 5: Statistical values: mean, standard deviation, minimum and maximum.

The average value gradually increases from -9.18 m for the raw data to -3.56 m in the "data D" set, indicating a shift in the distribution towards higher Z values. At the same time, the standard deviation rises, suggesting greater variability in the data across subsequent subsets. The minimum value remains relatively stable, oscillating around -12 m, while the maximum value across all sets is 47.69 m, indicating that the range of the data remains unchanged. Overall, the chart indicates a rising trend in the average value and an increasing range of data with subsequent sets.

In the next step, a visual analysis of the surfaces obtained from the sets was conducted using the Empirical Bayesian Kriging interpolation method. The first surface was created from the source data – prior to reduction (Figure 6).

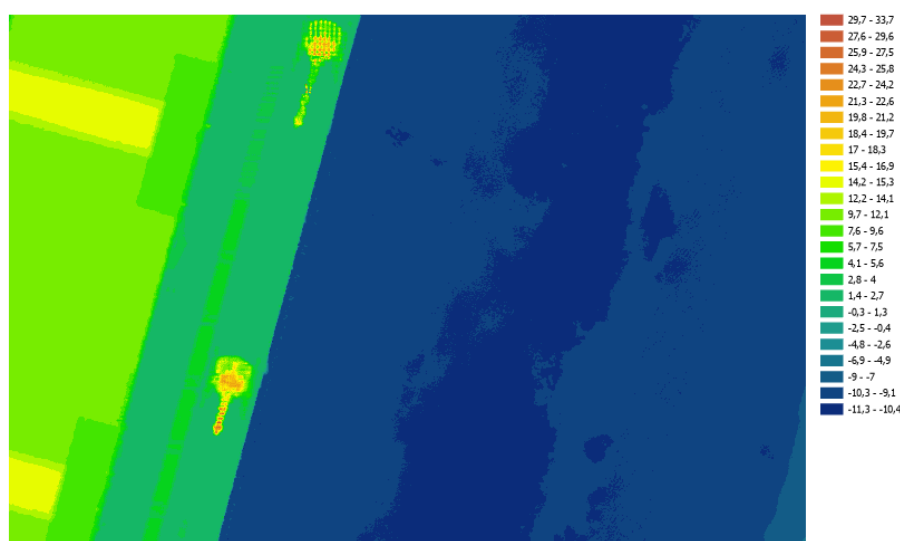


Figure 6: EBK surface created from raw data.



In the source model, the inclines are the most varied, especially in transitional areas between valleys and hills. Steep slopes and abrupt elevation changes are clearly visible. The terrain is rich in detail, with many local elevations and depressions. The surface is dynamic, indicating high resolution and accurate representation of the real terrain. The roughness is very high, meaning the surface has numerous fine irregularities and textures. These details are essential for analysing local structures and microforms of the landscape. The minimum and maximum elevations are well represented, with clear contrasts between the lowest and highest points. Locally, there are steep differences, for example, in areas of abrupt elevation changes. The following illustration shows the surface generated from reduced data – data A (Figure 7).

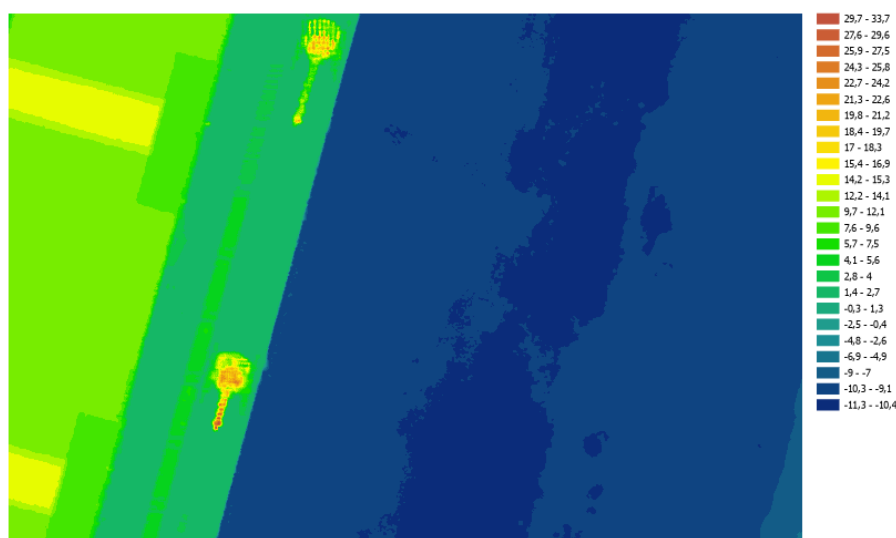


Figure 7: EBK surface created from data A.

320

The surface gradient is already averaged, but it still retains some of the original variation. The slopes are gentler than in the source surface, yet still noticeable. The surface is somewhat more uniform. The local terrain dynamics have been partially smoothed, but larger geographical features remain visible. The roughness has been reduced, especially in areas with small irregularities. The changes are less pronounced, particularly in areas with significant elevation differences. Local peaks and depressions have been smoothed, but differences in global Z values are still apparent. Figure 8 shows the surface created from dataset B.

325

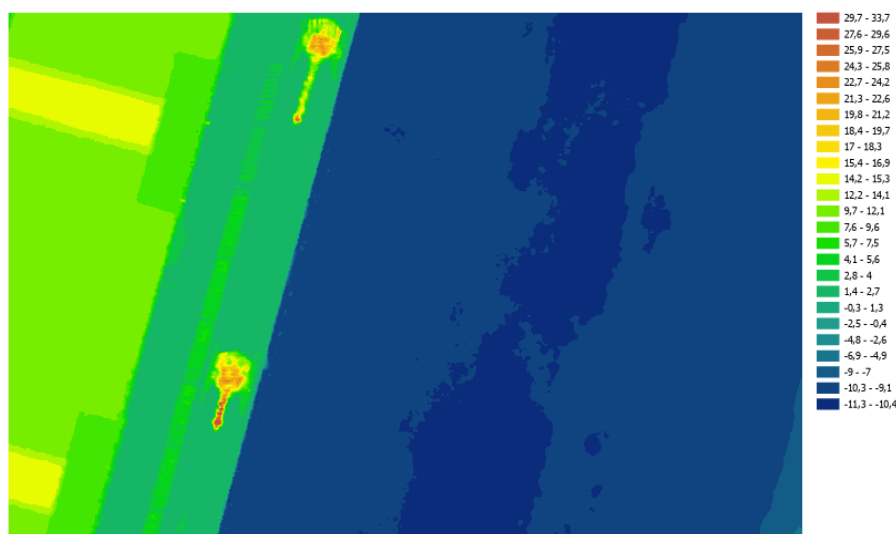


Figure 8: EBK surface created from data B.

330 The slope in this case is more averaged. The differences in slopes between adjacent pixels are smaller, which leads to the smoothing of steep slopes. The surface is even more uniform, resulting in the loss of some detailed geographical forms. The roughness is significantly reduced. Areas that were particularly uneven on the source surface are now smoothed out. Local peaks and depressions have been considerably averaged. The maximum and minimum Z values are less dynamic on a local scale, but still visible in larger structures. Figure 9 shows the surface created from the reduced data – data C.

335 .

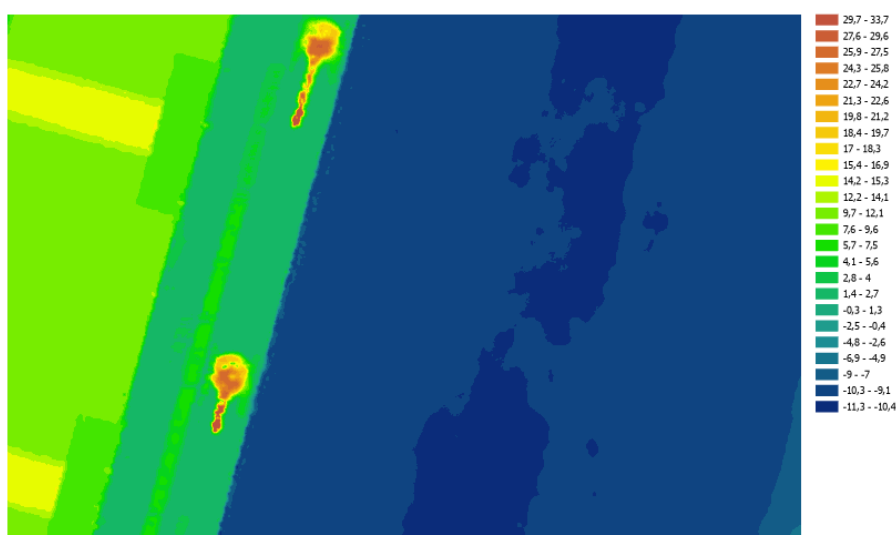


Figure 9: EBK surface created from data C.



In this case, the slopes are very gentle. Even in areas with originally steep banks, the surface has been smoothed to gentle
340 transitions. The terrain is highly averaged, significantly losing most local geographical forms. Only large structures are
visible. The roughness is very low, which means that the surface is smooth and devoid of minor irregularities. Local
differences in Z values have been almost completely reduced. Elevation differences are maintained only in large
topographical structures. The last visualisation presents the surface model for date D (Figure 10).

345

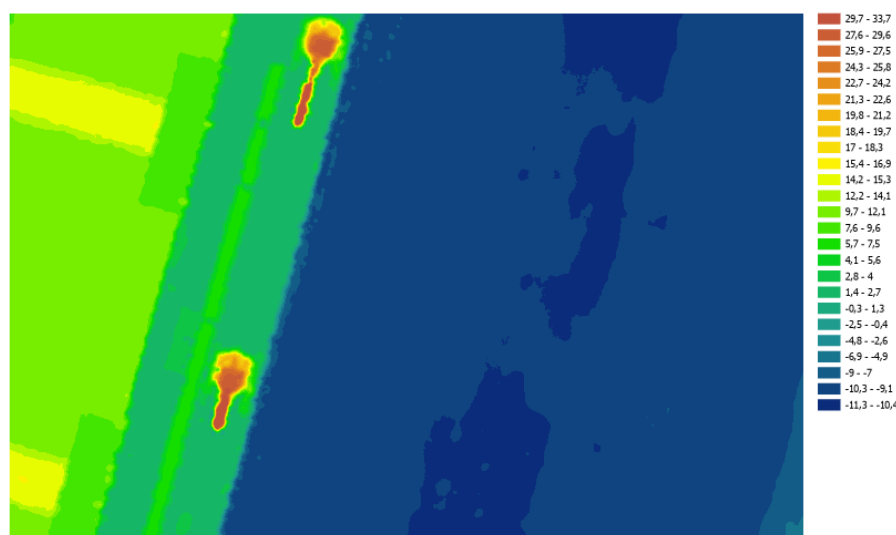


Figure 10: EBK surface created from data D.

The inclinations have been reduced to the greatest extent, and the surface has been simplified and averaged. The local terrain
350 dynamics have been diminished. The roughness is the lowest among all models. The maximum and minimum Z values are
preserved in a very simplified form, without local details.

The next analysis involves calculating and showing the surface difference. In Figure 11, we see a visualisation of the height
differences between the actual surface (derived from the raw data) and the four generalised surfaces. Each map has been
developed using a colour scale, which illustrates the height differences in metres relative to the source surface.

355

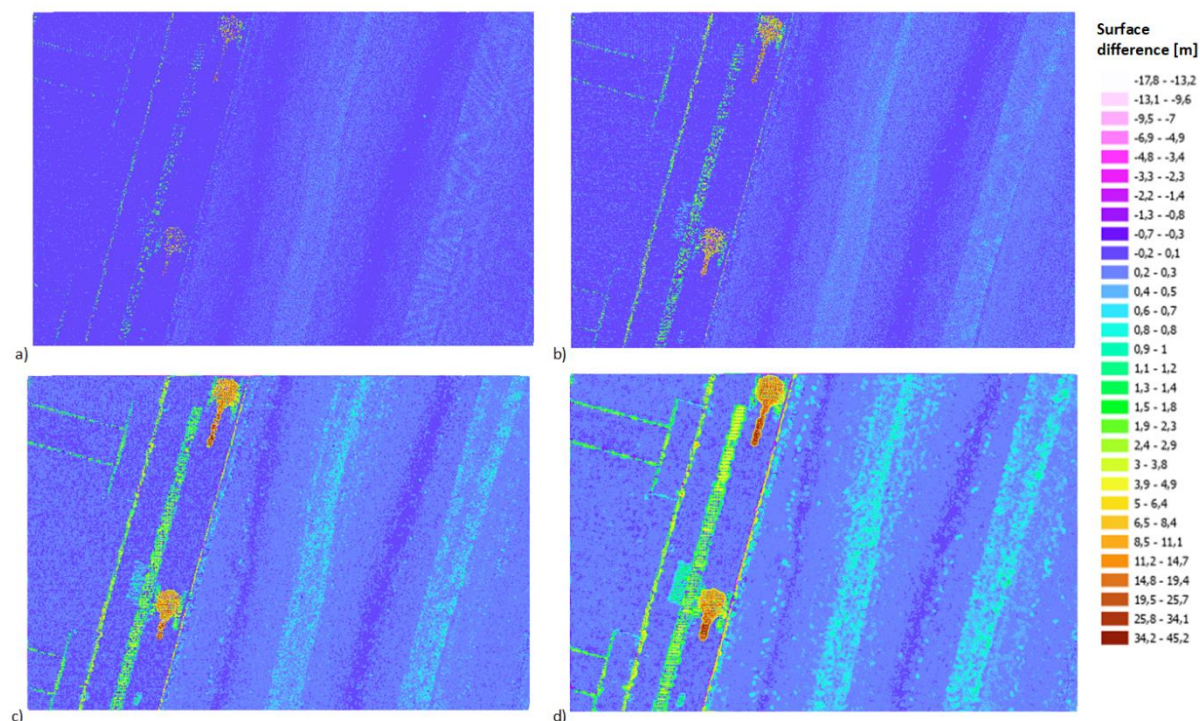


Figure 11: Surface difference: a) data A, b) data B, c) data C and d) data D.

The differences in height in metres are presented in the form of a colour gradient: shades of purple represent differences from -17.8 m to -3.4 m (areas with the greatest depressions compared to the actual surface), shades of blue represent differences from -3.3 m to -0.3 m (smaller depressions, close to the actual surface), shades of green represent differences from -0.2 m to 1.2 m (the best match to the actual surface, with differences close to zero), while shades of yellow, orange, and red represent differences from 1.3 m to 45.2 m (areas where the generalised surface is clearly elevated compared to the actual surface). The surface created from data A shows the smallest differences in height, which is a consequence of a low level of generalisation. The details of the terrain's shape, such as small irregularities and roughness, are clearly visible. The slopes are gentle, indicating a high degree of similarity to the actual surface. The surface generated from data B is more simplified than A, resulting in greater differences in height. Small landforms become less distinct. In steeper areas, noticeable differences in elevations and depressions can be observed. The slope increases in certain places, suggesting a less accurate representation of the more inclined terrain fragments. The surface created from data C shows significantly greater height differences, due to a higher degree of generalisation. A clear reduction in small landforms is evident. The surface becomes more smoothed, leading to a loss of detail. The slope becomes more uniform, especially in places with large height differences. The final surface is the least precise, with the greatest height differences. The surface is the most smoothed, with a clear simplification of landforms. Details such as depressions and small elevations have been entirely reduced.



In the next stage, the surface difference function was used to calculate the differences between the two surfaces in three ranges: -1 below (the first surface is lower than the second), 0 the same (no changes in height), and 1 above (the first surface is higher than the second). The surfaces for the aforementioned ranges of change were determined and the volume calculated accordingly. Additionally, the percentage range of changes was presented. All results are shown in Table 2.

Table 2. Differences between the source surface (raw) and the surfaces were created from reduced data.

| | Data A | Data B | Data C | Data D |
|---------------|------------------------|-------------------------|-------------------------|-------------------------|
| Area for -1 | 736,98 m ² | 970,58 m ² | 608,68 m ² | 303,36 m ² |
| Area for 0 | 4837,42 m ² | 1892,29 m ² | 33,96 m ² | 0,44 m ² |
| Area for 1 | 9417,16 m ² | 12128,65 m ² | 14347,83 m ² | 14685,41 m ² |
| Area for -1 | 4,92% | 6,47% | 4,06% | 2,02% |
| Area for 0 | 32,27% | 12,62% | 0,23% | 0,00% |
| Area for 1 | 62,82% | 80,90% | 95,71% | 97,97% |
| Volume for -1 | 40,68 m ³ | 119,71 m ³ | 128,06 m ³ | 111,54 m ³ |
| Volume for 1 | 936,84 m ³ | 1966,48 m ³ | 4350,81 m ³ | 6683,84 m ³ |

At the outset, it is important to mention that the area for the entire region amounts to 14989,21 m² and the volume to ground level is 6795.38 m³. In the table, we see the total land areas for each class of elevation differences, the percentage share of each class's area relative to the total area of the analysed region, and the volume differences with respect to the actual surface area. The areas vary in terms of generalisation level, which is reflected in the distribution of area and volume across the individual classes. Areas of class -1, indicating areas below the actual surface, gradually decrease with increasing generalisation, reaching a value of 736.98 m² (4.92%) for surface A and 303.36 m² (2.02%) for surface D. Class 0, denoting areas that perfectly match the actual surface, also shows a decline—from 32.27% for surface A to just 0.23% and 0.00% for surfaces C and D, which reflects a significant simplification of the terrain due to generalisation. Areas of class 1, corresponding to surface areas above the actual, show the opposite trend—their share increases from 62.82% for surface A to as much as 97.97% for surface D. Similarly, the volume for class 1 rises significantly with generalisation, from 936.84 m³ for surface A to 6,683.84 m³ for surface D. In contrast, the volume for class -1 is relatively small, reaching its maximum for surface C (128.06 m³). The analysis indicates that an increase in the level of generalisation leads to a significant simplification of the surface, resulting in a reduction of depressions (class -1) and areas consistent with reality (class 0), while simultaneously increasing the area above the actual surface (class 1). This process highlights terrain elevations and eliminates minor landforms, which may be useful in larger-scale analyses, but is less precise in modelling the details of the terrain.



Attention should also be drawn to the time required for creating surfaces using the EBK method. For the raw data, the computer took over nine hours to create a surface with a resolution of 0.1m. In contrast, for the reduced data, it needed only 4 minutes and 51 seconds (for data A), and the resulting surfaces differ little from one another. This indicates the significance of data reduction.

5 Conclusion and Discussion

This article makes a significant contribution to the development of spatial data processing methods by proposing a new approach to analysing data from two different sensors used in the coastal zone – LiDAR and multi-beam echosounder (MBES). Traditional approaches to hydrographic and bathymetric data processing typically focus on a single data source, which limits their ability to comprehensively represent dynamic coastal areas. This study combined and integrated data from both measurement systems, enabling a more thorough analysis of the topography and bathymetry of the coastal zone. A key element of the research was the development of a proprietary method for spatial data reduction based on Self-Organising Maps (SOM) neural networks. This method was initially developed for analysing bathymetric data but was optimised within this study for processing waterborne data, allowing effective application to both LiDAR and MBES measurement points. The algorithm adjustment for both positive and negative values in elevation and depth data enabled efficient and precise processing of large sets of spatial information, representing a significant expansion of the existing applications of this method.

The analysis results demonstrated that the proposed method significantly reduces the number of measurement points while preserving key features of the terrain surface. The optimisation for waterborne data facilitated effective processing in areas where traditional approaches often lose accuracy due to high topographic variability and the diversity of structures occurring in the coastal zone (e.g., the shoreline, embankments, port infrastructure).

Additionally, the comparative analysis of the interpolated surfaces showed that data reduction significantly shortens processing time without a significant loss in the quality of the final topographic and bathymetric models. The application of the Empirical Bayesian Kriging (EBK) method to the reduced data allowed for a reduction in surface generation time from over 9 hours (for raw data) to just 4 minutes and 51 seconds (for reduced data – data A), highlighting the importance of data optimisation in the analysis of spatial big data.

The conducted research has shown that the application of artificial intelligence to the analysis of spatial data from the coastal zone allows for effective optimisation of information processing processes, particularly in the context of large datasets (spatial big data). The proprietary reduction method based on Self-Organising Maps (SOM) enabled a significant decrease in the number of measurement points without a substantial loss of key surface features. This reduction impacted the statistics of the datasets, as can be observed in the increasing value of the mean Z and the rising standard deviation in the subsequent subsets. This indicates that the process primarily eliminated points with lower values, resulting in a more diverse dataset.



One of the key results is the statistical analysis presented in the results table. The original dataset (raw data) consisted of 2,168,011 points, with a mean height/depth value of -9.18 m, and a relatively low standard deviation of 4.16 m. Subsequent stages of reduction showed that with fewer points, both the mean value and the standard deviation increase – for the most reduced dataset (Data D, 18,107 points), the mean was -3.56 m, and the standard deviation rose to 9.14 m. This suggests a selective removal of lower values, resulting from the difference in the amount of data derived from LiDAR and MBES systems.

The results of surface interpolation using Empirical Bayesian Kriging (EBK) demonstrated that the greater the reduction, the greater the loss of terrain details. Visualisations of surface difference in ArcGIS Pro showed that surfaces generated from data with a higher degree of reduction exhibited increasingly larger differences from the raw data. Areas with significant height differences (e.g., port cranes, quays) were most susceptible to errors related to the generalisation of surfaces. Increasing the level of reduction led to a gradual smoothing of the model and the elimination of minor terrain structures.

The study provides significant insights into the possibilities of optimising spatial data processing using artificial intelligence methods. Contemporary measurement systems, such as LiDAR and MBES, generate vast amounts of data that require advanced analysis and reduction methods to be practical. In the scientific context, the research findings confirm the effectiveness of machine learning algorithms in spatial analysis and indicate the need for their further development to improve the accuracy of topographic and bathymetric models.

From the perspective of practical applications, efficient data reduction is crucial in various fields, such as hydrography, marine engineering, environmental management, and monitoring of port infrastructure and coastal zones. The developed method allows for the optimisation of analyses in GIS systems, enabling faster and more efficient processing and visualisation of results. This makes it possible to more effectively monitor environmental changes, identify threats (e.g., coastal erosion), and plan activities related to the management of port and marine areas.

Processing spatial data on a big data scale represents one of the key challenges in contemporary geoinformatics. As measurement technologies develop, not only do the possibilities for gathering information increase, but so too do the difficulties related to storing, analysing, and visualising that information. Bathymetric data, such as that obtained through MBES, can amount to hundreds of millions of points, making their processing highly resource-intensive. The developed reduction method significantly alleviates the burden on GIS systems, allowing for more efficient processing and analysis. Reducing spatial data in the context of spatial big data not only conserves computational resources but also enhances the interpretation of results by eliminating redundant points and focusing analysis on key terrain structures. In practice, this translates to better optimisation of 3D models, streamlined simulation processes, and reduced demand for computational power in remote sensing and GIS analyses. The study confirms that appropriately selected AI methods can significantly improve the efficiency of working with spatial data, and their integration with classical interpolation methods (e.g., EBK) allows for the creation of high-quality terrain models while maintaining essential details.

Although the proposed data reduction method brings significant benefits, it also has certain limitations. The biggest challenge is finding a balance between data reduction and the loss of essential information about the terrain's topography.



The analysis of surface differences has shown that with reduction, there is a gradual smoothing of the model and the removal of minor elements, which can affect the accuracy of the final analyses.

Another limitation is the fact that the applied SOM and EBK methods are dependent on initial parameters. The choice of the neural network topology, the size of the neighbourhood, or the number of iterations is crucial for the final shape of the reduced dataset. There is a risk that with suboptimal parameters, the reduction may lead to excessive loss of detail or the retention of unnecessary outliers.

The study has shown that the application of AI methods in the reduction of spatial data is an effective solution for the challenges associated with spatial big data. The integration of SOM and EBK methods allows for the optimisation of bathymetric and topographic data analysis, which is significant for both science and engineering practice. Further development of these technologies opens new possibilities in the management of spatial data and their effective interpretation in the context of global environmental changes. Importantly, the data after reduction meet the requirements of the International Hydrographic Organization (IHO) regarding the accuracy of bathymetric measurements for shallow water bodies. This means that the developed method allows for the optimisation of hydrographic analysis without compromising international data quality standards, making it an effective solution for seabed mapping and coastal area management.

6 Challenges and future directions

In the future, it is worthwhile to focus on further optimisation of reduction methods to minimise the loss of key terrain features while maintaining high efficiency in data processing. One potential direction is the use of advanced deep learning algorithms, which can automatically adjust reduction parameters to the specific nature of the area being analysed.

An additional area of research could be the integration of reduction methods with cloud technologies and real-time analysis systems, which would allow for dynamic processing of big spatial data in applications related to environmental monitoring and maritime navigation. It would also be valuable to explore the possibility of combining data reduction methods with temporal trend analysis, which would enable more effective forecasting of environmental changes in coastal zones.

Another significant challenge is computational complexity and resource demand. Although methods based on artificial intelligence, such as Self-Organising Maps (SOM), significantly reduce the amount of data, the initial processing and training of AI models require substantial computational resources, especially in the case of deep learning-based approaches. Future research should focus on optimising AI algorithms to reduce the demand for computational power and processing time, which would enable their implementation in applications operating in real time or on cloud GIS platforms.

Another significant issue is the scalability and adaptability of AI methods to different geographical regions and datasets. AI models trained on specific bathymetric data may not perform as well in new environments due to differences in topography, sediment dynamics, or hydrodynamic conditions. Future innovations should focus on adaptive learning techniques that allow AI models to autonomously adjust to newly acquired spatial data, minimising the need for manual fine-tuning of algorithms. Furthermore, the development of hybrid AI models that combine classic geostatistical methods (e.g., Empirical Bayesian



Kriging) with machine learning algorithms could enhance data processing accuracy even further. Hybrid models can
495 leverage the strengths of traditional interpolation techniques and the AI's ability to recognise patterns in data, enabling more
precise and flexible spatial analyses.

The results of the conducted research highlight the potential of AI in streamlining monitoring and management of coastal
zones. The application of AI methods in spatial data processing can significantly increase the accuracy and efficiency of
hydrographic surveys, reducing the time and resources required for large-scale mapping. Maritime administrations,
500 environmental protection agencies, and port managers could utilise AI techniques to model changes in coastal zones, which
would enable proactive decision-making in response to climate-related threats, such as rising sea levels, coastal erosion, or
the degradation of marine habitats.

The use of artificial intelligence in spatial data processing represents a breakthrough in hydrographic analysis and coastal
zone management. However, to fully exploit its potential, it is necessary to address issues related to data quality,
505 computational requirements, and the interpretability of AI models.

References

- Asan, U., Ercan, S. (2012). An Introduction to Self-Organizing Maps. In: Kahraman, C. (eds) Computational Intelligence
Systems in Industrial Engineering. Atlantis Computational Intelligence Systems, vol 6. Atlantis Press, Paris.
https://doi.org/10.2991/978-94-91216-77-0_14
- 510 Augustijn, EW., Zurita-Milla, R. Self-organizing maps as an approach to exploring spatiotemporal diffusion patterns. *Int J
Health Geogr* **12**, 60 (2013). <https://doi.org/10.1186/1476-072X-12-60>
- Biernacik, P.; Kazimierski, W.; Włodarczyk-Sielicka, M. Comparative Analysis of Selected Geostatistical Methods for
Bottom Surface Modeling. *Sensors* 2023, **23**, 3941. <https://doi.org/10.3390/s23083941>
- Christensen, J. H., Mogensen, L. V., & Ravn, O. (2020). Deep learning based segmentation of fish in noisy forward looking
515 MBES images. *IFAC-PapersOnLine*, **53**(2), 14546-14551.
- Contarinis, S., and Kastrisios, C. (2022). Marine Spatial Data Infrastructure. The Geographic Information Science &
Technology Body of Knowledge (1st Quarter 2022 Edition), John P. Wilson (Ed.). DOI: 10.22224/gistbok/2022.1.6.
- DiPaola, F., Bhardwaj, A., & Sam, L. (2023). Generating an interactive online map of future sea level rise along the North
Shore of Vancouver: methods and insights on enabling geovisualisation for coastal communities. *arXiv preprint*
520 *arXiv:2304.07469*.
- Foglini, F., Rovere, M., Tonielli, R., Castellan, G., Prampolini, M., Budillon, F., Cuffaro, M., Di Martino, G., Grande, V.,
Innangi, S., Loreto, M. F., Langone, L., Madricardo, F., Mercorella, A., Montagna, P., Palmiotto, C., Pellegrini, C., Petrizzo,
A., Petracchini, L., Remia, A., Sacchi, M., Sanchez Galvez, D., Tassetti, A. N., and Trincardi, F.: A new multi-grid
bathymetric dataset of the Gulf of Naples (Italy) from complementary multi-beam echo sounders, *Earth Syst. Sci. Data*, **17**,
525 181–203, <https://doi.org/10.5194/essd-17-181-2025>, 2025.



- International Hydrographic Organization (IHO), 2023. Spatial Data Infrastructures: The Marine Dimension, 3rd ed. Monaco: IHO. Available at: https://iho.int/uploads/user/pubs/cb/c-17/C-17%20Ed%203.0.0_October%202023_Final.pdf [Accessed 29 Jan. 2025].
- Irish J.L., White T.E., Coastal engineering applications of high-resolution lidar bathymetry, Coastal Engineering, Volume 35, Issues 1–2, 1998, Pages 47-71, ISSN 0378-3839, [https://doi.org/10.1016/S0378-3839\(98\)00022-2](https://doi.org/10.1016/S0378-3839(98)00022-2).
- Kang, Y., Gao, S., & Roth, R. E. (2024). Artificial intelligence studies in cartography: a review and synthesis of methods, applications, and ethics. *Cartography and Geographic Information Science*, 1-32.
- Lugga, M. S. (2025). Integrating Artificial Intelligence (AI) with Geographic Information Systems (GIS) and Remote Sensing Technologies for Security Management. *Direct Research Journal of Engineering and Information Technology*, 13(1), 1–6. <https://doi.org/10.26765/DRJEIT547398281>
- Minelli, A., Tassetti, A. N., Hutton, B., Pezzuti Cozzolino, G. N., Jarvis, T., & Fabi, G. (2021). Semi-Automated Data Processing and Semi-Supervised Machine Learning for the Detection and Classification of Water-Column Fish Schools and Gas Seeps with a Multibeam Echosounder . *Sensors*, 21(9), 2999. <https://doi.org/10.3390/s21092999>
- Mujta, W.; Włodarczyk-Sielicka, M.; Stateczny, A. Testing the Effect of Bathymetric Data Reduction on the Shape of the Digital Bottom Model. *Sensors* 2023, 23, 5445. <https://doi.org/10.3390/s23125445>
- NV5 and NOAA, 2025. NV5 and NOAA will mark 20 years of collaboration on geospatial projects mapping nation's coasts and waterways during Coastal GeoTools 2025. *LiDAR Magazine*, 21 January 2025. Available at: <https://lidarmag.com/2025/01/21/nv5-and-noaa-will-mark-20-years-of-collaboration-on-geospatial-projects-mapping-nations-coasts-and-waterways-during-coastal-geotools-2025/> [Accessed 29 Jan. 2025].
- Le Deunf, J., Debese, N., Schmitt, T., & Billot, R. (2020). A Review of Data Cleaning Approaches in a Hydrographic Framework with a Focus on Bathymetric Multibeam Echosounder Datasets. *Geosciences*, 10(7), 254. <https://doi.org/10.3390/geosciences10070254>
- Papakonstantinou, A., Topouzelis, K., and Pavlogeorgatos, G. (2016). Coastline Zones Identification and 3D Coastal Mapping Using UAV Spatial Data. *ISPRS International Journal of Geo-Information*, 5(6), 75. <https://doi.org/10.3390/ijgi5060075>
- Poenicke, O., Mandal, C., & Treuheit, N. (2023). Lidar and AI Based Surveillance of Industrial Process Environments. *Transport and Telecommunication Journal*, 24(1), 1-10.
- Rane, J., Kaya, O., Mallick, S. K., Rane, N. L. (2024). Artificial intelligence-powered spatial analysis and ChatGPT-driven interpretation of remote sensing and GIS data. In *Generative Artificial Intelligence in Agriculture, Education, and Business* (pp. 162-217). Deep Science Publishing. https://doi.org/10.70593/978-81-981271-7-4_5
- Qian, Y., Forghani, M., Lee, J. H., Farthing, M., Hesser, T., Kitanidis, P., & Darve, E. (2020). Application of deep learning-based interpolation methods to nearshore bathymetry. *arXiv preprint arXiv:2011.09707*.
- Specht, M., & Wiśniewska, M. (2024). A Method for Developing a Digital Terrain Model of the Coastal Zone Based on Topobathymetric Data from Remote Sensors. *Remote Sensing*, 16(24), 4626. <https://doi.org/10.3390/rs16244626>



- 560 Tripathi, K. (2024). The novel hierarchical clustering approach using self-organizing map with optimum dimension selection. *Health Care Science*, 3(2), 88–100. <https://doi.org/10.1002/hcs2.90>
- Vitousek S, Buscombe D, Vos K, Barnard PL, Ritchie AC, Warrick JA. The future of coastal monitoring through satellite remote sensing. *Cambridge Prisms: Coastal Futures*. 2023;1:e10. doi:10.1017/cft.2022.4
- Wright, D.J. (2009). Spatial Data Infrastructures for Coastal Environments. In: Yang, X. (eds) Remote Sensing and
- 565 Geospatial Technologies for Coastal Ecosystem Assessment and Management. Lecture Notes in Geoinformation and Cartography. Springer, Berlin, Heidelberg. https://doi.org/10.1007/978-3-540-88183-4_5
- Yarger, D., Stoev, S., & Hsing, T. (2022). A functional-data approach to the Argo data. *The Annals of Applied Statistics*, 16(1), 216–246.
- Zaresefat, M., Derakhshani, R., & Griffioen, J. (2024). Empirical Bayesian Kriging, a Robust Method for Spatial Data
- 570 Interpolation of a Large Groundwater Quality Dataset from the Western Netherlands. *Water*, 16(18), 2581. <https://doi.org/10.3390/w16182581>
- Zhang, F., Tan, T., Hou, X., Zhao, L., Cao, C., & Wang, Z. (2024). Underwater Mapping and Optimization Based on Multibeam Echo Sounders. *Journal of Marine Science and Engineering*, 12(7), 1222. <https://doi.org/10.3390/jmse12071222>
- Zhao, Q., Pepe, A., Zamparelli, V., Mastro, P., Falabella, F., Abdikan, S., Calò, F. (2023). Innovative remote sensing
- 575 methodologies and applications in coastal and marine environments. *Geo-Spatial Information Science*, 27(3), 836–853. <https://doi.org/10.1080/10095020.2023.2244006>

Author Contributions: Conceptualization, M.W.-S.; methodology, M.W.-S.; software, M.W.-S.; validation, M.W.-S.; formal analysis, R.D.; investigation, M.W.-S.; resources, M.W.-S.; data curation, M.W.-S.; writing—original draft

580 preparation, M.W.-S.; writing—review and editing, M.W.-S. and R.D.; visualization, M.W.-S.; project administration, M.W.-S.; funding acquisition, M.W.-S.

Funding: This research was funded by the National Science Centre, Poland (NCN) under grant MINIATURA 8 no. 2024/08/X/ST10/00291.

585

Acknowledgments: This research was funded in whole by the National Science Centre, Poland (NCN) under grant MINIATURA 8 no. 2024/08/X/ST10/00291. For the purpose of Open Access, the authors have applied a CC-BY public copyright license to any Author Accepted Manuscript (AAM) version arising from this submission.